

Article

Investigation of Icelandic Dust Presence in the Aerosols Collected at Hornsund (Svalbard, Norwegian Arctic) in Spring 2019

Beatrice Moroni ^{1,*} , Stefano Crocchianti ¹, Adam Nawrot ^{2,3} , Pavla Dagsson Waldhauserova ^{4,5}  and David Cappelletti ^{1,6} 

¹ Department of Chemistry, Biology and Biotechnology, University of Perugia, 06123 Perugia, Italy; croc@impact.dyn.unipg.it (S.C.); david.cappelletti@unipg.it (D.C.)

² Institute of Geophysics, Polish Academy of Sciences, 01-452 Warsaw, Poland; anawrot@igf.edu.pl

³ forScience Foundation, 87-100 Toruń, Poland

⁴ Faculty of Environmental and Forest Sciences, Agricultural University of Iceland, 311 Hvanneyri, Iceland; pavla@lbhi.is

⁵ Faculty of Environmental Sciences, Department of Water Resources and Environmental Modeling, Czech University of Life Sciences Prague, 165 00 Prague, Czech Republic

⁶ Institute of Polar Science (CNR-ISP), 40129 Bologna, Italy

* Correspondence: b.moroni@tiscali.it

Abstract: An integrated morphological and chemical analysis of Arctic aerosols was undertaken for Icelandic dust and Svalbard aerosols to be compared by scanning electron microscopy coupled with EDS microanalysis (SEM–EDS) via imaging and chemical analysis techniques. Results of the characterization of the particles from both surface sediments and suspended dust from desert areas in Iceland confirmed that volcanic glass is an excellent marker of Icelandic dust origin. Classification diagrams of particle chemical composition clearly distinguished the volcanic glass particles from the local surface sediments at Hornsund, Svalbard. In the same diagrams, a few particles were found in the aerosols from Hornsund which were morphologically and chemically similar to the Icelandic volcanic glass particles. Such properties, in principle, cannot be considered exclusive to volcanic glass. However, since Iceland is the largest and the most active source of long-range transported dust in the northern European high latitudes, and air mass trajectories reaching Hornsund did, actually, pass Iceland before the aerosol collection in the period under consideration, these particles likely originated in Iceland. On the other hand, the comparison with local and Icelandic sediments revealed the presence in the aerosols from Hornsund of particle types that cannot be attributed to either local or Icelandic dust. This observation highlights the possibility of extending and validating the application of the proposed geochemical criterion to different dust sources across the Arctic and the sub-Arctic, provided a consistent geochemical databank of representative dust sources from these areas is arranged.

Keywords: Icelandic dust; aerosol particles; sediment samples; scanning electron microscopy; mineral chemistry; provenance; Arctic region



Citation: Moroni, B.; Crocchianti, S.; Nawrot, A.; Dagsson Waldhauserova, P.; Cappelletti, D. Investigation of Icelandic Dust Presence in the Aerosols Collected at Hornsund (Svalbard, Norwegian Arctic) in Spring 2019. *Atmosphere* **2024**, *15*, 322. <https://doi.org/10.3390/atmos15030322>

Academic Editor: Jean-Christophe Raut

Received: 3 February 2024

Revised: 29 February 2024

Accepted: 1 March 2024

Published: 4 March 2024



Copyright: © 2024 by the authors. Licensee MDPI, Basel, Switzerland. This article is an open access article distributed under the terms and conditions of the Creative Commons Attribution (CC BY) license (<https://creativecommons.org/licenses/by/4.0/>).

1. Introduction

Dust emissions at high latitudes and in cold climates (Iceland, Greenland, Svalbard, Alaska, Canada, Russia, Scandinavia, New Zealand, Patagonia, and Antarctica) have been widely recognized as driving the local climate, biological productivity, and air quality (e.g., [1–7]). In the Northern Hemisphere, high-latitude dust, with its wide range of morphological and chemical properties, can induce significant direct (blocking sunlight) and indirect (through clouds and cryosphere) radiative climate forcing [8,9] through solar radiation fluxes and snow optical characteristics, strongly impacting Arctic amplification and the resulting glacier melt [1,10]. Glacial meltwater supplies the glacial outwash plains

with tens of centimeters of new fine sediments in a single flood. If glacial lagoons are not created on the glacier tongue outlets, new silty surfaces are exposed to weathering and aeolian processes, leading to increasing dust emissions, having significant effects on the environment and climate [1,11].

Iceland is Europe's largest source of aeolian dust [12]. Iceland includes large desert areas in continuous evolution due to the combined action of volcanic eruptions and surface erosion by glacial, wind, and fluvial actions according to the season and the topographical location of the exposed surfaces. Volcanic eruptions occur every 3–4 years on average and provide new material for particle suspension, usually removed from the surface with strong winds in less than one year [13]. However, not all eruptions are explosive, as per none of the past four eruptions reported in Iceland from 2014 to 2023. Desert areas with high wind erosion rates cover >40% of Iceland [12]. The most significant contribution to dust emission comes from three 'superactive' dust hot spots in ice-proximal areas: Dyngjúsandur in NE Iceland, Myrdlassandur, and Landeyjarsandur in southern Iceland.

Long-term weather observation since the 1940s (SYNOP codes for dust) has shown that there are about 135 dust days annually in Iceland [14,15]. April to October is the period of the most intense dust production/emission in NE Iceland, while dust is emitted year-round, with the highest rates in March–June, in the southern part of Iceland. In many cases, dust rising in Iceland is a limited and short-lived phenomenon, such as dust devils, but in some cases, it evolves to severe dust storms [16]. April to May is often the time in which the combination of dust storms and northward transport of air masses to the High Arctic typically occurs [2–4,6]. An estimate of 4–40 million tons of Icelandic dust contributing to aerosols at high latitudes every year places Iceland among the most active high-latitude dust (HLD) sources [1,2,17]. Furthermore, the extent of the contribution from Iceland to the dust Arctic aerosol pool is expected to increase in the future due to the deglaciation affecting this and other dust sources at high latitudes in response to climate change.

The possible occurrence of Icelandic dust in the Arctic atmospheric air has already been reported [2,3,18]. In aerosols collected in Svalbard, such presence was first demonstrated by Moroni et al. [4,19], who documented the presence, in aerosols sampled at Ny-Alesund, of metal oxides and volcanic glass particles compatible with the tholeiitic Icelandic magmatic system. However, the broader application of such tracers remains to be confirmed elsewhere. Therefore, the present work aimed to verify the existence and effective usefulness of such mineralogical–geochemical markers of Icelandic origin in the long-range dust transported to Hornsund, SW Svalbard. This location has long been the subject of studies on climate, glaciology, and geomorphology in the High Arctic environment, but only recently has it hosted studies on the chemical composition and dust concentration of the snowpack [20–24]; studies on dust and aerosol composition in Hornsund are, still, rare and do not comprise mineral chemistry and dust composition [25,26]. The possibility of sampling aerosols, snow, and sediments during the same campaign in Hornsund provided the opportunity to conduct different studies (e.g., [24]), including this one. The period considered in this study is that of April–May 2019, in which the occurrence of intense dust storm phenomena in Iceland has been established and documented.

2. Background, Samples, and Methods

The composition of local (from the Hornsund area) and Icelandic surface sediments was analyzed and then compared to the composition of atmospheric aerosol particles from Hornsund. Aerosol samples were collected in spring, when snow cover is present at Hornsund [27], which limits the local dust input onsite. Sediments, dust, and aerosols were all analyzed by scanning electron microscopy with energy-dispersive spectrometry (SEM–EDS) focused on individual silicate and metal oxide Fe-bearing particles. These particles were chosen for their ability to discriminate aerosols from different sources (e.g., Iceland rather than Greenland or North Europe), and also because they are easily identifiable by SEM analysis due to their excellent contrast in backscattered electron imaging. Triangular plots of individual particle composition were developed for the local and Icelandic sediments

and then applied to characterize atmospheric dust particles in the aerosols from Hornsund to check for their provenance.

2.1. The Potential Dust Sources

2.1.1. Dust Sources in Iceland

Iceland is a highly active desert area with seven ‘superactive’ dust hot spots where up to 40 million tons of dust is suspended annually [12]. There are 135 dust days reported annually in Iceland and dust travels thousands of km inside the Arctic and >3500 km towards Europe [4,14,28]. The Icelandic dust sources investigated in this paper are the largest and most active deserts in Iceland: Dyngjusandur in the NE Iceland and Myrdalssandur in South Iceland (Figure 1a). Dyngjusandur is an about 140 km² large glacio-fluvial plain with suspension-prone silty sediments left on the surface after daily summer floods. Jökulhlaups occur often, bringing materials from the Bárðarbunga and Kverkfjöll volcanic systems. Sand sources are buried hyaloclastite ridges beneath Vatnajökull, while only large-sized plagioclase crystals in sands might be derived from the lava flows [29]. Dyngjusandur sand is composed of volcanic glass (80–90%), pyroxene, olivine, and plagioclase. It has a homogeneous composition typical of tholeiitic basalts with rather low TiO₂, Na₂O, and K₂O.

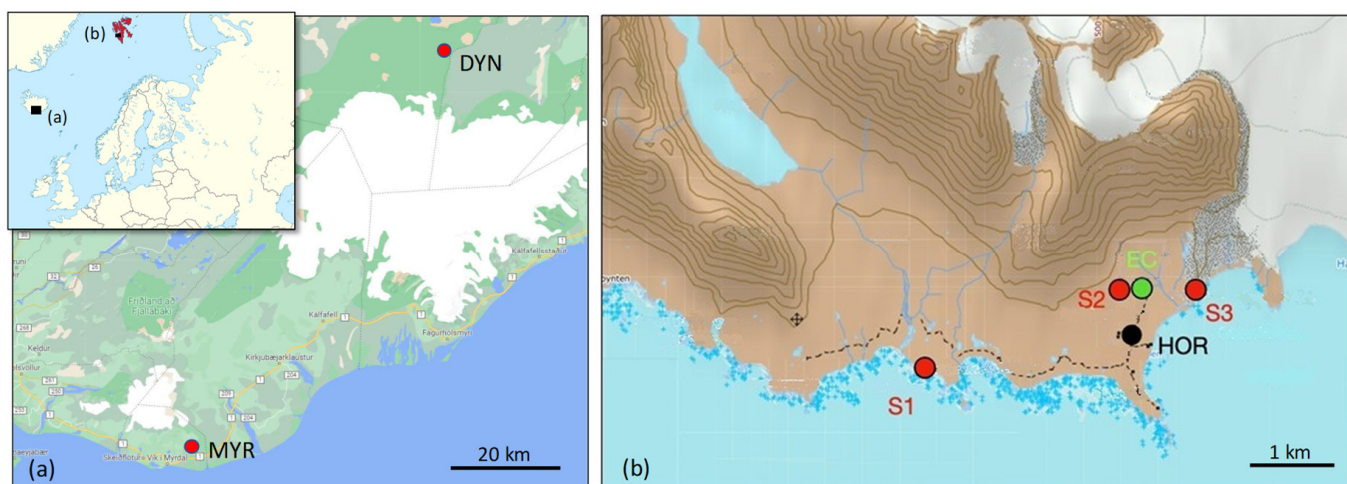


Figure 1. Maps of Iceland (a) and Svalbard (b) with locations of the sampling sites.

Myrdalssandur is an about 60 km² large glacio-fluvial lowland plain with basaltic unstable silty sediments from jökulhlaups of the Katla volcanic system [12]. The dominating mineral phase in Myrdalssandur dust is aluminosilicate glass (90%), followed by plagioclase, pyroxene, and olivine. It has relatively high Fe₂O₃ and TiO₂ contents [9]. The tholeiitic nature of the volcanic products in the two areas emerges from the composition dominated by volcanic glass, followed by augite and plagioclase in approximately equal quantities, and from variable, but generally low, amounts of Fe(Ti)-bearing spinel. Quartz and K-feldspars are not typical of the Icelandic atmospheric dust. However, the occurrence of K-feldspar was noted in the dust experimentally generated from the surface soil from one locality in Iceland [9].

2.1.2. Dust Sources in the Hornsund Area

Hornsund is the name of a fjord located in the southern part of the island of Spitsbergen (Svalbard archipelago), part of the South Spitsbergen National Park. Since 1957, the Polish Polar Station Hornsund (PSPH) has been operating in Isbjornhamna Bay. Since 1977, PSPH has been working all year round collecting, i.e., weather data. The weather station is located about 300 m from the coastline, on a coastal plain called Fuglebergsletta. This unglaciated area with minor denivelations stretches about 1000 to 2000 m from the coast (Figure 1b). Approximately 1000 m east of the PSPH, Fuglebergsletta meets the high moraines of the

Hansbreen Glacier, forming a natural boundary between the tide-water glacier (Hansbreen) and the marine terraces (up to 25 m of height), which extend 4.5 km westwards and then northwestwards. Fuglebergsletta is open to westerly winds that bring air masses from the ocean to the land.

The geology of the northwestern part of Hornsund Fjord is dominated by the Hecla Hoek Succession, which consists of gneisses, schists, amphibolites, phyllites, marbles, quartzites, and conglomerates [30,31]. Geologically, the Fuglebergsletta belongs to the Arikammen and Skoddefjellet Formations.

The Arikammen Formation consists of carbonate-mica schists, paragneisses (Skoddefjellet type), and minor interbedded marble layers [32]. The carbonate-mica schists are characterized by the mineral assemblage calcite + quartz + biotite + garnet + plagioclase + muscovite ± epidote, with Ca-enriched plagioclase and tourmaline, apatite, zircon, monazite, epidote group minerals, titanite, ilmenite, hematite, pyrite, pyrrhotite, and chalcopyrite as accessory minerals. Some schist varieties contain rare meionite [33]. Paragneisses with garnets contain plagioclase with andesine composition, calcite, clinozoisite, and Ca-scapolite [34].

The Skoddefjellet Formation consists of paragneisses and mica schists enriched in garnets [34]. Typical mineral assemblages are quartz + plagioclase + biotite + muscovite ± garnet ± chlorite [33]. Common accessory phases are similar to the Arikammen Formation plus sphene, allanite, xenotime, and magnetite [32]. Half of the rocks are phyllosilicate-rich with homogeneous flake gneisses and half of the rocks are feldspar-bearing quartzites (mica-poor). The meta-arenites contain quartz, plagioclase, biotite, muscovite, and almandine garnet. A distinctive feature is the remarkable presence of K-feldspar and oligoclase, which account for up to 50% of the mineralogical composition.

The snow accumulation period occurs in Hornsund between October and May, but, usually, a stable snow cover remains from January to June [27]. Only in specific areas, such as steep mountain slopes, the coastline, and hills, including moraines, can the snow be blown away, leaving the ground without snow cover. This fact points to these areas as potential active dust sources. However, the occurrence of dust uplift phenomena from these areas has not been documented for the period from March to May. Other studies focused on snow chemistry [20], aerosol particles [25], and pollution [22–24] also indicate sources located, e.g., in Iceland, Russia, and Europe. Snow sampling in an altitude profile on Arikammen Ridge, Hornsund, at the beginning of the ablation season revealed a clear negative correlation between dust deposition and elevation, suggesting that from elevations above 300 m above sea level, dust may consist more of long-range dust than at lower elevations, where local dust is more prevalent [21].

2.2. Air Mass Transport Modeling with Applications

Air mass backtrajectories (BTs) were calculated using the NOAA ARL HYSPLIT 5.1.0 transport model [35]. GDAS meteorological input fields with $0.5^\circ \times 0.5^\circ$ resolution and a propagation time of 240 h were employed. The trajectories were calculated from 10 April 2019, 00:00, to 14 May 2019, 23:00, for every hour and the endpoint altitudes 50, 500, 1000, and 3000 m a.g.l. at the Hornsund coastal area (77.00° N, 15.54° E). This fairly high resolution was employed due to the considerably long propagation time, while the final heights of the trajectories were selected to evaluate the impact of numerical artefacts. Four areas of interest were identified where the BT passage was enumerated. These areas corresponded to the administrative borders (Version 3.0.0 of 10 m—Natural Earth Admin 1—States, Provinces; <https://www.naturalearthdata.com/downloads/10m-cultural-vectors/10m-admin-1-states-provinces/> (accessed on 3 August 2023)) of Iceland (adm0_a3 = ISL), Great Britain and Ireland islands (adm0_a3 = GBR + IRL), Greenland (adm0_a3 = GRL) and Russia (adm0_a3 = RUS). An additional area, named Regional, corresponding to a rectangle (72.0° N, 32.2° E– 84.0° N, 6.0° E) containing the Svalbard archipelago and having a circular hole centered at Hornsund with a diameter of 5° , was defined. The hole in the Regional area allowed evaluation of the local contribution without

including the receptor location due to the convergence of the trajectories at the site. To count the trajectories per day crossing the five areas at a maximum altitude of 800 m a.g.l. using an accuracy of $0.5^\circ \times 0.5^\circ$, a Fortran code was written.

2.3. Sampling

Surface sediment samples from Iceland were collected on 20 and 26 August 2020 in a dedicated sampling campaign carried out as part of an inDust COST ACTION project [36]. The samples were collected in the Dynjusandur (hereafter DYN) and Myrdalssandur (hereafter MYR; Figure 1 and Table 1) deserts. Dust-lifting events from desert surfaces occurred, both at DYN and at MYR, during sampling so that it was also possible to take some samples of aeolian dust in the same places as the sediment samples. Mineral dust sampling at different height and distance from the place of origin was performed using both a cyclone for personal respirable dust sampling (GS-3, SKC, Eighty Four, PE, USA; 50% cut-point of 4 μm) operated at 2 L/min (AirChek[®] XR5000 Sample Pump, SKC, Eighty Four, PE, USA) on nucleopore polycarbonate membranes (Whatman, \varnothing 25 mm, porosity 0.1 μm), and a passive deposition chamber consisting of a plastic box with four gridded side walls housing four Petri dishes (8 cm diameter) as collector plates (Figure 2). In particular, MYR 1, MYR 1d, and D6 were collected at some distance from the dust events, whereas MYR 2 and D5b were collected in the middle of the storms. Duration of dust sampling is reported in Table 2.

Table 1. List of sediment, dust, and aerosol samples from Iceland and Hornsund.

Sample	Latitude	Longitude	Type/Sampling Time
MYR 1	63°29'20.2" N	018°46'47.1" W	dust/273 min
MYR 1a	63°29'20.2" N	018°46'47.1" W	Sediment
MYR 1b	63°29'20.2" N	018°46'47.1" W	Sediment
MYR 1d	63°29'20.2" N	018°46'47.1" W	dust/273 min
MYR 2	63°30'53.0" N	018°39'51.8" W	dust/35 min
DYN 1–5	64°54'8.3" N	016°39'4.15" W	Sediment
DYN 5b	64°54'8.3" N	016°39'4.15" W	dust/30 min
DYN 6	64°54'8.3" N	016°39'4.15" W	dust/30 min
S 1	76°59'53.9" N	015°27'56.2" E	Sediment
S 2	77°00'13.5" N	015°32'37.7" E	Sediment
S 3	77°00'17.4" N	015°33'34.0" E	Sediment
HOR 1–13	77°00'20.9" N	015°32'46.5" E	aerosol *

* Sampling time for aerosols is reported in Table 2.

Table 2. List of aerosol samples with sampling time and sampled air volume. Location Hornsund, Svalbard, 2019.

Sample Name	Sampler Start (UTC)		Sampler Stop (UTC)		Air Volume (m ³)
HOR 1	14 April	17:15	15 April	unknown	1.00
HOR 2	17 April	9:13	17 April	17:13	5.61
HOR 3	23 April	12:40	23 April	20:40	4.17
HOR 4	24 April	20:00	25 April	8:00	8.91
HOR 5	26 April	17:00	27 April	5:00	6.42
HOR 6	28 April	17:45	29 April	8:45	5.86
HOR 7	2 May	16:30	3 May	7:30	13.4
HOR 8	3 May	17:00	4 May	17:00	21.5
HOR 9	4 May	21:10	5 May	21:10	11.5
HOR 10	5 May	21:55	6 May	21:55	21.5
HOR 11	6 May	23:55	8 May	00:25	11.1
HOR 12	9 May	1:37	10 May	2:16	21.3
HOR 13	10 May	9:35	11 May	9:35	10.7

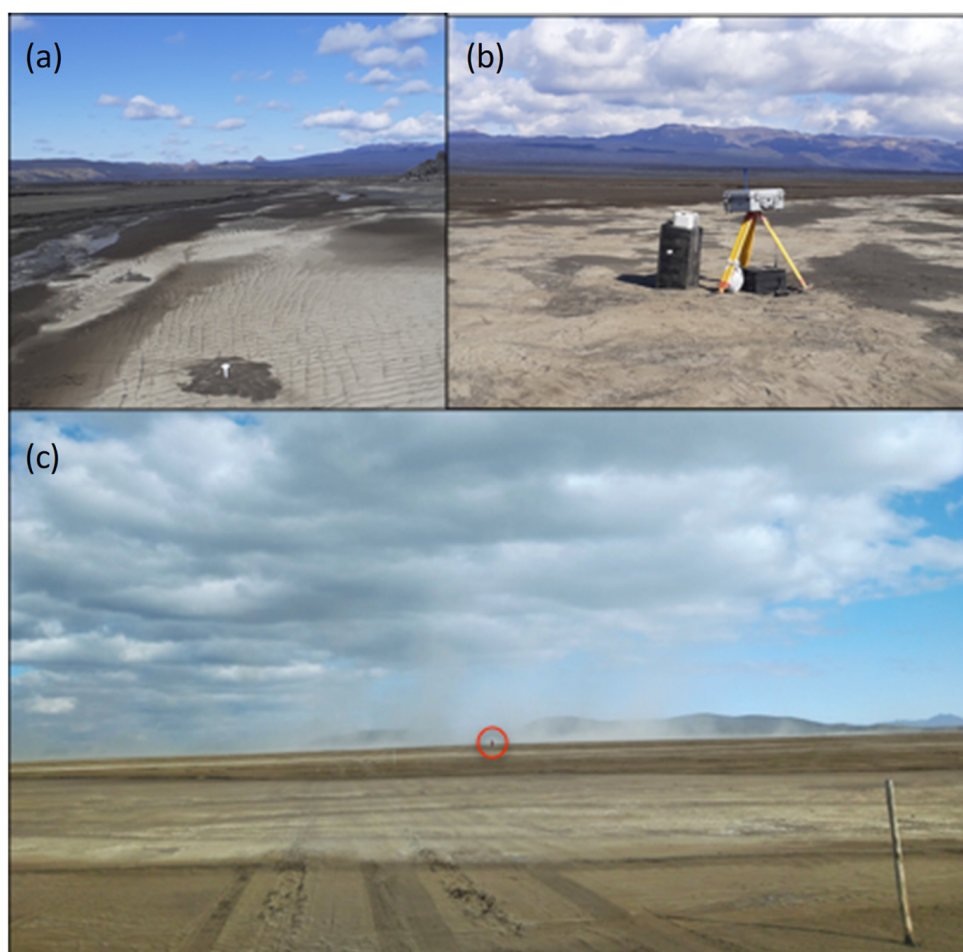


Figure 2. Sediment (a) and suspended dust (b,c) samplings at Dynjusandur (DYN), Iceland. The red circle marks the operator while performing personal sampling. Peak dust concentrations of $400 \mu\text{g m}^{-3}$ were captured by the DustTrak monitor, but the concentrations were likely significantly higher in the center of the dust storm.

The sampling campaign at Hornsund took place between 14 April and 11 May 2019 and involved the sampling of aerosols and the collection of surface sediments from snow-free ground areas. The aerosol sampling took place at the environmental chamber (EC in Figure 1) located approximately 500 m northeast of the Polish Polar Station Hornsund main buildings, using a sampler (Life 1 Mega System low-volume sampler, provided by Marek Michalik, Jagiellonian University, Cracow, Poland) operated at 15 L/min with polycarbonate filters (diameter 47 mm, porosity $0.1 \mu\text{m}$ or $0.2 \mu\text{m}$, alternating). The sampling was discontinuous and with variable duration. Sampling started on 14 April, it was temporarily stopped due to the occurrence of a rainy period between 17 and 23 April (see [24]), and proceeded until 10 May (Table 2). Duration of sampling was increasing in length from 8 h at the beginning in April to 24 h in early May, for a better chance of capturing detectable aerosol concentrations on the filters. Sampled air volumes fell in the range of 4.17 to 21.5 m^3 . Surface sediment sampling took place on 11 May and involved three locations (S1 to S3 in Figure 1b) at the same altitude, but at different distances from the aerosol sampling hub (HOR in Figure 1b). A list of Icelandic and Hornsund surface sediment, dust, and aerosol samples, with exact location and main characteristics, is shown in Table 1. The sampling times and air volume sampled at Hornsund are reported in Table 2.

After sampling the membrane, filters were stored in plastic boxes at room temperature before being subjected to SEM–EDS investigation. At that moment, they were stored in Petri dishes in a desiccator before and after coating.

2.4. Scanning Electron Microscopy

Individual particle analyses were performed by scanning electron microscopy coupled with energy-dispersive X-ray microanalysis (SEM–EDS). The loose sediment samples were prepared by mounting a small aliquot of the sediment directly onto double-sided carbon tape fixing it upon the stub. The dust and the aerosol samples were prepared by cutting single portions ($\sim 10 \times 10$ mm) from the central part of the polycarbonate sampling filters and mounting them on to SEM aluminum stubs using the double-sided carbon tape. Both sample types were finally coated with a 100–150 Å carbon film to provide electrical conductivity and prevent charge build-up during the exposure to the electron beam.

Scanning electron microscopy imaging was performed using a Supra 25 microscope (ZEISS, Oberkochen, Germany) equipped with a field emission gun and a GEMINI column employed at a variable voltage (0.5–15 kV) and magnification (500 to 350,000 \times) to distinguish particle types and textural details. The instrument is also equipped with an X-ray-dispersive spectrometer (QUANTAX EDS microanalysis system coupled with ESPRIT 2.2 software for data treatment; Bruker Corp., Billerica, MA, USA). EDS spectra (spot size 5, working distance 8.5 mm) were collected for 90 s and the elemental composition obtained after standardless matrix correction provided by the ESPRIT software. Values lower than 0.1 wt% (SEM detection limit) were omitted. After preliminary observation and identification of the grain types, a total number of 30–40 grains per sample were analyzed.

3. Results and Discussion

3.1. Characteristics of Sediment, Dust, and Aerosol Samples

Icelandic surface sediment samples consisted of variably sorted and abraded sand. The more the sediments were weathered and fluvially transported, the higher their sorting and average grain size, the more rounded the grains, and the fewer fresh surfaces they showed. All these characteristics point to variable intensity and/or duration of sedimentary processes by surface waters in jökulhlaups.

The composition of both MYR and DYN sediments was dominated by volcanic glass (Figure 3). Rietveld quantitative X-ray diffraction analysis on the same samples confirmed these observations, providing 80–85 wt% and 60–80 wt% of amorphous phase, i.e., volcanic glass, in the two sites, respectively (Moroni, personal communication). The larger glass fragments were spheroidal or botryoidal in shape and vesicular in appearance with inclusions of the other phases. The smaller glass fragments, instead, were splinters of irregular shape. Plagioclase, pyroxene, and metal-bearing minerals followed the volcanic glass in this order of abundance. The plagioclase particles, of various sizes and quite fresh-looking, mostly showed andesine to labradorite compositions. Pyroxenes consisted of enstatite and augite; they were generally euhedral and were found included in the glass fragments. The metal-bearing minerals (mostly Fe–Cr-spinel, ilmenite, titanite, and iron sulfide as accessory phase) were also included in the glass fragments. Representative SEM–EDS microanalyses of mineral and glass particles in the Icelandic sediment samples are shown in Table 3a.

No significant differences were observed in the type or composition of sediments, nor between sediments and resuspended dust, in the MYR and DYN sample set. The only small differences found were due to the effects of erosion–transport–sedimentation mechanisms active in the same place. This was the case, for example, of the whitish surface crusts observed on the crests of the jökulhlaups erosion channels (e.g., Figure 2a), in which a larger presence of fine-grained granules and less-dense phases, such as plagioclase and glass, was found.

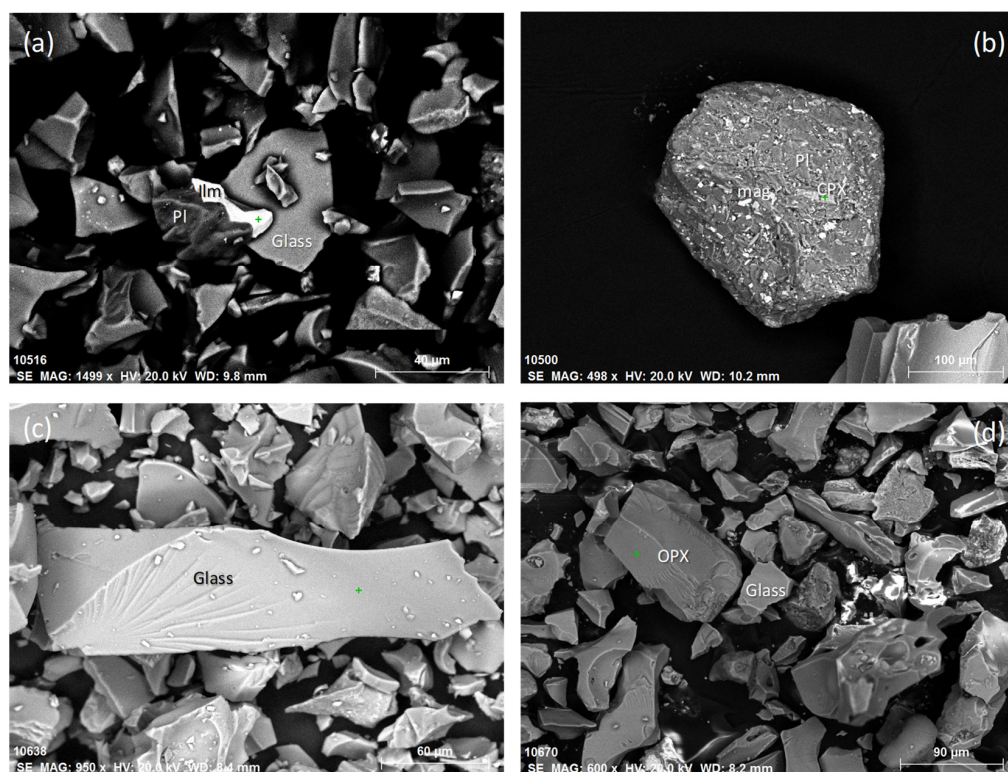


Figure 3. Scanning electron microscopy, secondary electron micrographs of representative phases in MYR sediment (a), MYR dust (b), DYN sediment (c), and DYN dust (d) samples. Acronyms: Pl, plagioclase; Ilm, ilmenite; mag, magnetite; CPX, clinopyroxene; OPX, orthopyroxene. MYR—Myrdahlsandur, Iceland; DYN—Dynjusandur, Iceland.

Compared to the Icelandic sediments, the sediments from Hornsund were much more mature, with rounded and abraded grains. The grain size was coarse, with a general range of variation from $<5 \mu\text{m}$ to $>200 \mu\text{m}$ and a different degree of sorting in different samples (Figure 4). While samples S1 and S3 consisted of loose sediments (Figure 4a,c), sample S2 (Figure 4b) showed the characteristics of a dark vegetated soil, rich in humus, with few residual quartz and alkali feldspar grains. The composition of the sediments (Table 3b) consisted of quartz, feldspar (K-feldspar and low-Ca plagioclase), chlorite, and mica (typically biotite). The accessory minerals were zircon (sediment samples S1 and S3), iron sulfide, phosphates (apatite and monazite in soil S3), and iron oxides (sediment sample S3). The mineralogical association was perfectly consistent, both in terms of typology and abundance of minerals, with the metamorphic rocks outcropping in the surroundings of the Polish Polar Station.

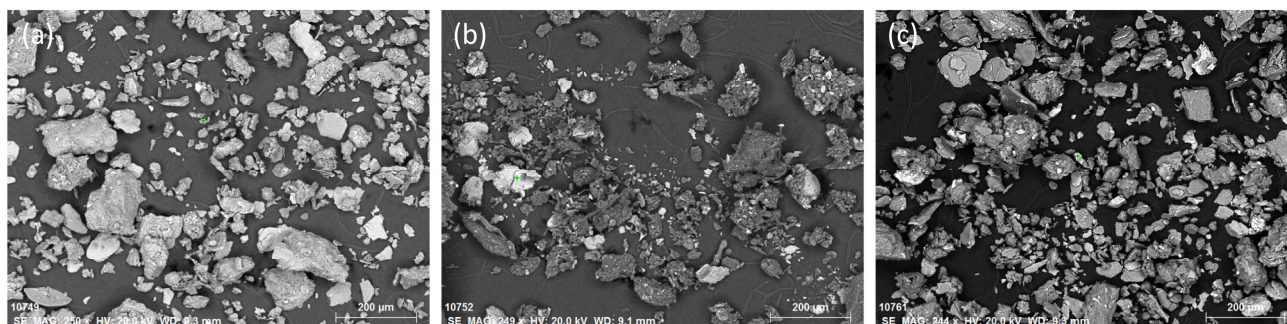


Figure 4. Scanning electron microscopy, secondary electron micrographs of representative phases in sediment samples S1 (a), S2 (b), and S3 (c) in Hornsund, Svalbard.

Table 3. Representative chemical analyses (wt %) of individual particles in the sediment samples from Iceland and Hornsund area (a) and in the aerosol samples from Hornsund (b).

(a)												
SAMPLE label	M1a 10516b	D6 10688	M1a 10516a	M1 10463	M1d 10505a	M1a 10516	M1a 10523	D6 10695c	S1 10743d	S1 10743c	S2 10757	S3 10773
Type	glass	glass	plagioclase	enstatite	augite	metal oxide	metal oxide	titanite	biotite	plagioclase	plagioclase	chlorite
Oxygen	48.48	51.30	50.54	60.92	45.64	12.64	21.05	60.81	46.87	49.66	53.10	52.28
Sodium	2.78	2.56	4.39	0.00	0.35	0.07	0.67	0.00	0.82	4.80	10.12	0.94
Magnesium	3.55	2.61	0.37	17.62	7.64	0.44	1.63	0.54	6.88	0.61	0.40	6.68
Aluminium	7.09	7.86	14.95	1.28	0.82	1.82	1.87	1.76	9.94	15.81	10.40	12.21
Silicon	17.84	20.53	20.43	19.12	18.81	2.90	4.22	8.26	14.61	21.12	25.08	8.91
Phosphorus	0.22	0.14	0.00	0.00	0.00	0.00	0.03	0.00	0.00	0.09	0.08	0.00
Sulfur	0.00	0.00	0.00	0.00	0.00	0.00	0.00	0.00	0.00	0.07	0.10	0.00
Potassium	0.46	0.44	0.24	0.00	0.00	0.04	0.12	0.00	4.39	0.31	0.34	0.20
Calcium	6.67	5.04	8.11	0.00	11.15	0.57	1.14	13.23	0.68	7.06	0.00	0.00
Titanium	2.45	1.43	0.09	0.00	0.61	15.26	29.47	13.63	0.99	0.00	0.00	0.00
Iron	10.45	8.10	0.89	1.06	14.98	66.27	39.79	1.78	14.71	0.47	0.38	18.77
(b)												
SAMPLE label	HOR 1 9989	HOR 1 9966	HOR 1 9970	HOR 2 10012	HOR 2 10003a	HOR 3 10104	HOR 3 10107a	HOR 6 10165	HOR 7 10181	HOR 10 10263a	HOR 11 10277	HOR 13 10406
Type	chlorite	Pyroxene (?)	plagioclase	Glass (?)	Pyroxene (?)	biotite	chlorite	muscovite	chlorite	feldspar	plagioclase	muscovite
Oxygen	61.38	55.97	47.56	53.86	47.53	52.20	55.02	48.18	51.15	52.30	52.83	58.82
Sodium	2.37	2.12	7.66	6.17	0.00	0.00	0.96	0.00	1.63	0.72	10.25	2.48
Magnesium	11.27	10.22	0.00	8.86	6.28	2.97	6.07	1.44	2.72	1.75	0.00	0.76
Aluminium	9.58	3.88	13.89	5.42	3.36	8.12	11.92	18.69	17.11	7.85	11.06	8.63
Silicon	8.28	14.78	26.63	13.08	13.31	24.23	12.54	19.47	13.74	33.07	25.33	20.57
Phosphorus	0.00	0.00	0.00	0.24	0.00	0.00	0.00	0.00	0.00	0.00	0.00	0.00
Sulfur	0.00	0.00	0.00	0.11	0.00	0.00	0.00	0.00	0.15	0.00	0.13	0.19
Potassium	0.33	0.16	0.33	0.33	0.84	2.57	0.00	9.30	2.67	2.26	0.00	7.81
Calcium	0.00	6.82	3.92	5.12	10.68	0.00	1.00	0.00	0.00	0.00	0.41	0.00
Titanium	0.00	0.00	0.00	0.00	0.53	0.75	0.21	0.40	0.00	0.24	0.00	0.00
Iron	6.80	6.05	0.00	6.81	17.47	9.16	12.28	2.45	10.82	1.80	0.00	0.22

Natural particles were the main component in the aerosols from Hornsund. They showed a rich and varied composition given by silicates, sulfides, metal oxides, carbonates, phosphates, sulfates, and chlorides (Table 4). Silicates consisted of quartz, feldspars (mainly K-feldspar and albite), mica (biotite and, more rarely, muscovite/phengite), chlorite, and accessory titanite and zircon. A phase containing only Si and Al was also found, as a few dispersed grains, in samples HOR 5 and HOR 6. Rare individual crystals with shape and composition compatible with those of pyroxene were present in sample HOR 1 (see Figure 5a and Table 3b), while silicate grains with irregular shape and a composition compatible with those of volcanic glass were found in samples HOR 1 and HOR 2 (see Figure 5b and Table 3b). Grain size was fine to medium with a predominance of particles in the range 1–5 μm .

Table 4. Constituent minerals/phases in the aerosol samples (in order of abundance).

Sample	Mineral/Phase
HOR 1	Plagioclase, alkali feldspar, quartz, rutile, baryte, Mg-Ca-Fe silicate, mica, iron oxide, chlorite, dolomite, titanite
HOR 2	Chlorite, dolomite, plagioclase, iron oxide, Mg-Ca-Fe silicate, Fe-Ti oxide
HOR 3	Gypsum, mica, chlorite, plagioclase
HOR 4	Sodium chloride, gypsum, plagioclase
HOR 5	Alkali feldspar, gypsum, sodium chloride, mica, quartz, aluminum silicate
HOR 6	Mica, plagioclase, quartz, apatite
HOR 7	Chlorite, alkali feldspar, mica, iron oxide, sodium chloride, potassium chloride, (Na-)Ca sulfate, gypsum, dolomite
HOR 8	Chlorite, gypsum, baryte, Fe-Ti oxide
HOR 9	Sodium chloride, gypsum, mica, plagioclase
HOR 10	Sodium chloride, alkali feldspar, mica, iron sulfide, quartz, titanium oxide, apatite
HOR 11	Sodium sulfate, zircon, plagioclase, alkali feldspar, chlorite, apatite, titanite
HOR 12	Chlorite, mica, alkali feldspar, quartz, Na-Ca sulfate, Fe-Zn sulfide
HOR 13	Quartz, chlorite, gypsum, alkali feldspar, titanium oxide

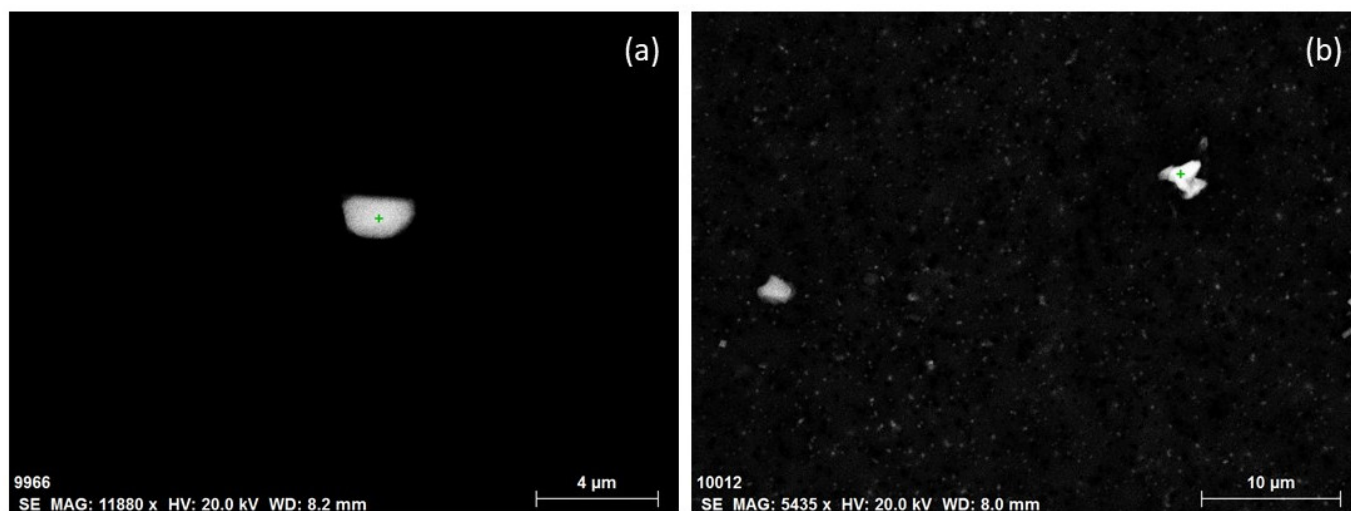


Figure 5. Scanning electron microscopy, secondary electron micrographs of individual particles with a composition compatible with that of (a) pyroxene, and (b) glass; chemical analyses of these particles are reported in Table 3b.

Among the other mineralogical species, the sulfides and the metal oxides contained iron and/or zinc/titanium, and the phosphates consisted of apatite and monazite, while carbonates (calcite and dolomite) were rare. The salts were represented by sodium and/or potassium chloride, along with calcium, sodium, and barium sulfate. The distribution (type, abundance) of the phases in the aerosol samples in the period of interest was not

homogeneous. In particular, the relative abundance of chlorides and sulfates was extremely low in aerosol samples HOR 1, HOR 2, and HOR 6, and high to very high in the rest of the samples (Table 4).

3.2. Comparing Aerosol Particles with Sediment Samples as Potential Source Material

In order to identify possible geochemical–mineralogical markers capable of distinguishing Icelandic from local dust sources, the compositions of the mineral particles in the Icelandic and Hornsund sediment and aerosol samples were compared. In the ternary diagram in Figure 6, the compositions of the types of particles representative of the different dust sources, namely, glass, plagioclase, pyroxene, and metal-bearing minerals for the Icelandic terrains, along with feldspar, mica, and chlorite for the Hornsund terrains, are reported. In the graph, the main particle types are quite well distinguishable from each other. Specifically, the glass, chlorite, and mica particles are located in three distinct areas of the graph, while the clinopyroxene (augite) lies in the range of chlorites. The metal-bearing and the orthopyroxene (enstatite) particles concentrate in the proximity of the upper vertex of the diagram, with no clear distinction between them, while feldspars are distributed along the line joining the other two components. The composition of the glass particles shows a wide range of variation in the content of both the alkali and alkaline earth metals (Na, K, and Ca) and the transition metals (Fe and Ti), but without appreciable differences between MYR and DYN, nor between surface sediments and dust. This demonstrates the general similarity of the characteristics of the sediments in the two dust sources in Iceland, along with the nonselectivity of the dust emission process. However, glass particles are well distinguishable from the other particle types, which confirms glass as a distinctive marker of the Icelandic origin of the dust [4].

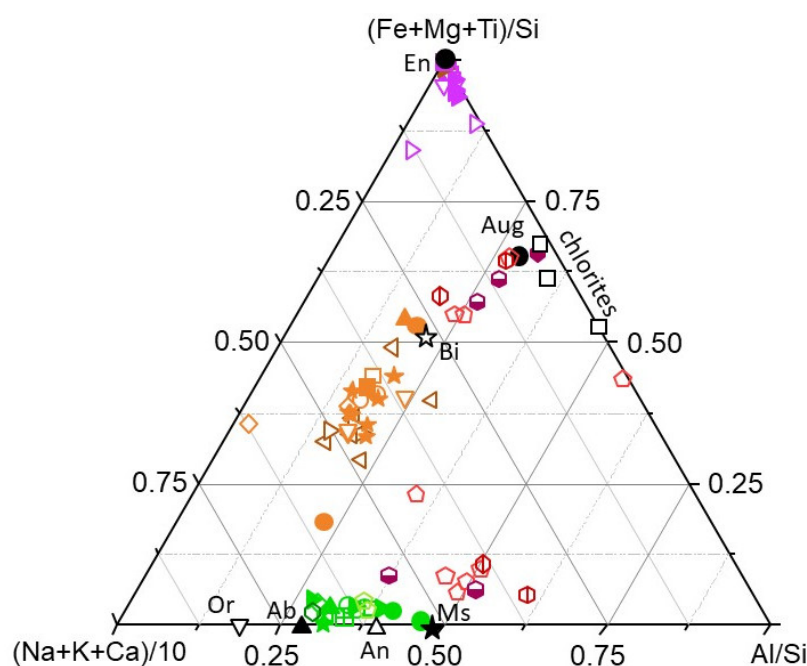


Figure 6. Ternary diagram of the composition of glass (orange), feldspar (green), metal oxides and silicates (violet), and the sheet silicate (mica and chlorite; red) particles in sediments (open and mid-open symbols) and dust (solid symbols) from Iceland and Hornsund (Svalbard). Symbols for samples: solid circles, M1; open circles, M1a; open squares, M1b; solid squares, M1d; solid up triangles, M2; open left triangles, D1; open right triangles, D2; open diamonds, D3; open down triangles, D5; solid right triangles, D5b; solid stars, D6; open pentagons, S1; open hexagons, S2; mid-open hexagons, S3. Acronyms: En, enstatite; Aug, augite; Bi, biotite; Or, orthoclase; Ab, albite; An, anorthite; Ms, muscovite.

The next step was to compare the composition of the local and Icelandic markers with that of the aerosol particles, in order to identify the possible presence of the Icelandic component in the Hornsund aerosol, and possibly to distinguish it from the local one. The graph in Figure 7 shows the results of comparison. Aerosol particles from Hornsund are distributed over the entire triangular diagram, with a prevalence of intermediate compositions. In this context, only five particles from the HOR 1 to HOR 6 (14 to 28 April) samples accumulate within the region occupied by glass particles (Figure 7a), while the greatest portion of them have compositions different from those of surface sediments and dusts used for comparison (Figure 7a,b). In the samples of 26 and 28 April (HOR 5 and HOR 6), we find, instead, some Al-rich particles absent in the May samples (Figure 7). At the two extremes of the transition metal contents, metal oxides and feldspars are represented in the entire period with some prevalence on 14 and 17 April.

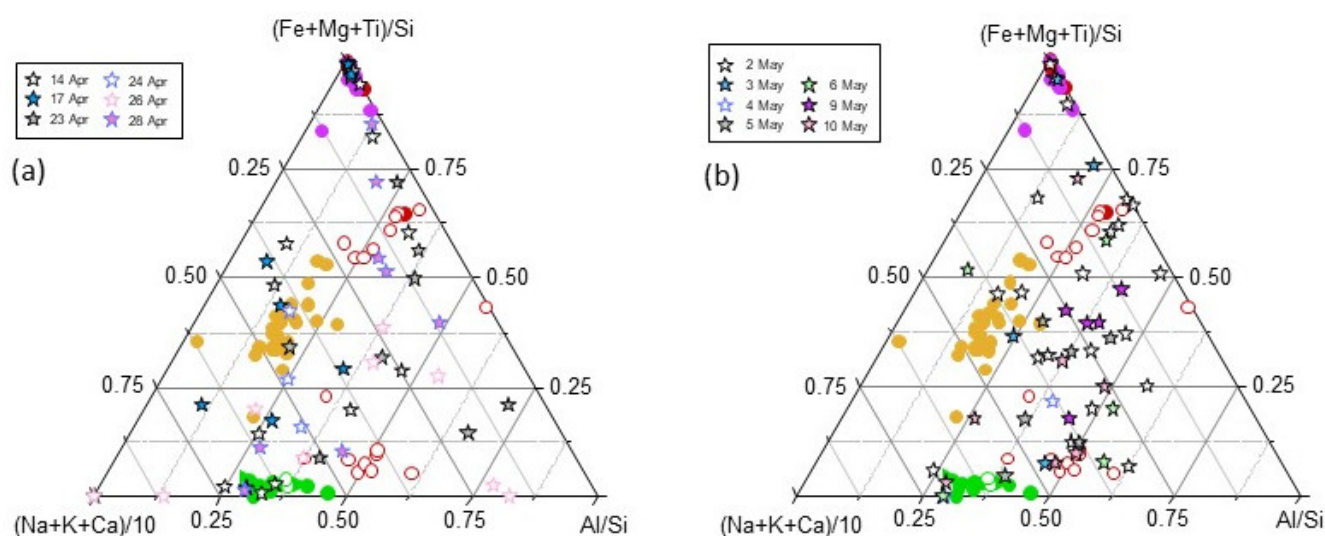


Figure 7. Ternary diagrams of the composition of the particles in the aerosols sampled in April (a) and May (b). The sediment and dust samples from Iceland (solid circles) and Hornsund (Svalbard; open circles) are reported for comparison. Symbols and colors are as in Figure 6, with no distinction in shape between ground sediments and resuspended dust.

3.3. Air Mass Transport to Hornsund and Dust Events in Iceland

In the period under consideration, the air masses reaching Hornsund came from different geographical areas, namely, Iceland, Greenland, North Europe, and/or the British Isles and Russia. In addition to this, the area was affected by a regional circulation involving the Arctic and/or Atlantic Ocean along with Svalbard (Figure 8). The extent of the contribution of the source areas changed significantly over time (Figure 9). In fact, before 14 April, most of the contribution to the air masses came from Greenland. After that date, the circulation rotated slightly eastwards, mainly towards Iceland and the British Isles. Since 20 April, a series of incursions of air masses from Russia was registered. This situation lasted until the end of April, with the exception of a new, high-altitude, weak incursion from Iceland between 24 and 26 April. The situation changed dramatically in May when most of the atmospheric circulation reaching the receptor site was from Eurasia and the Russian Arctic.

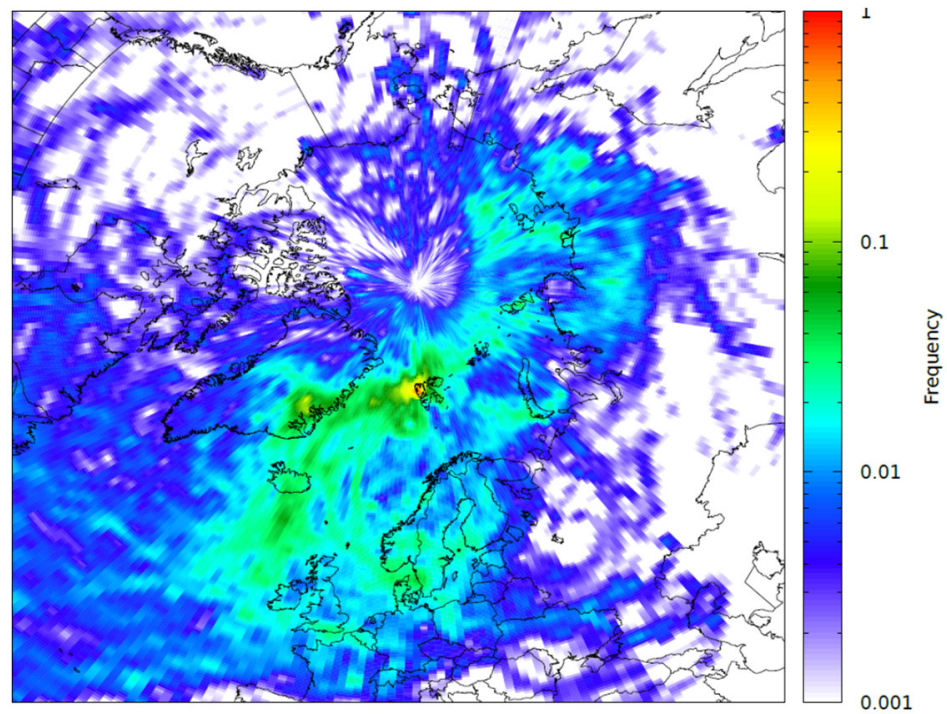


Figure 8. Frequency plot of the 960 backtrajectories reaching Hornsund at 500 m a.g.l. every hour from 10 April to 19 May 2019. Note the logarithmic scale to highlight areas far from the converging point.

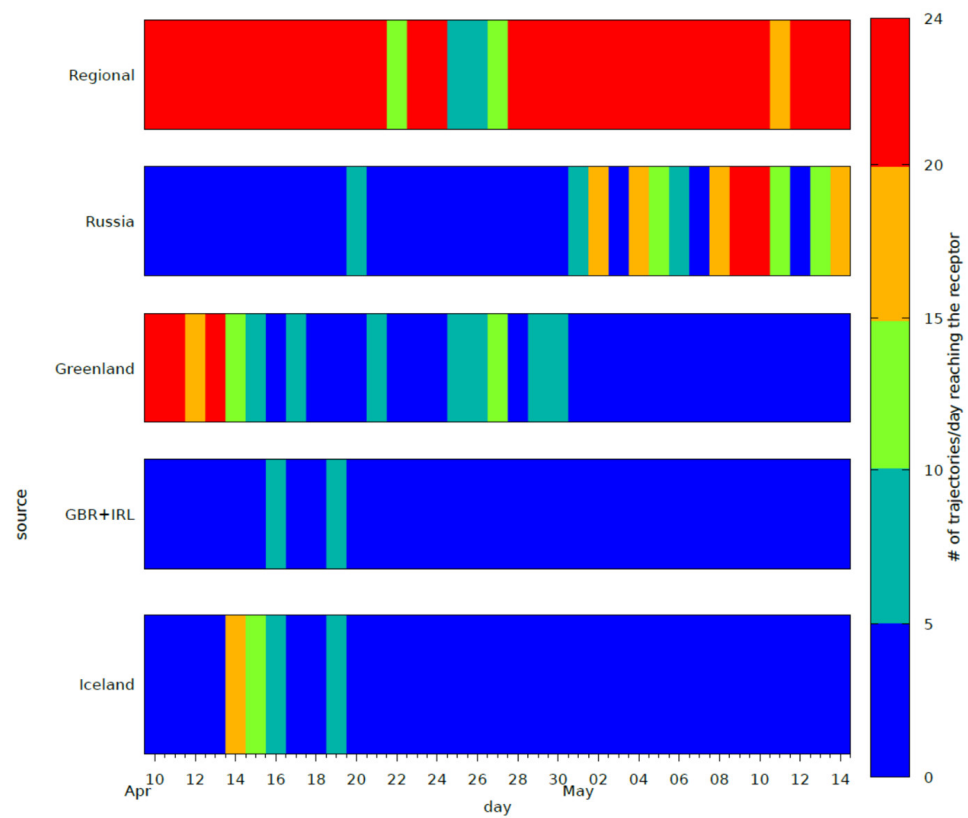


Figure 9. Heatmap of the number of trajectories per day reaching Hornsund at whole hours at the altitude of 500 m a.g.l. and crossing the areas of Iceland, Great Britain and Ireland islands, Greenland, Russia, and the additional Regional one (72.0° N, 32.2° E–84.0° N, 6.0° E) below 800 m a.g.l.

Meteorological data collected by the Polish Polar Station Hornsund show that the wind direction (measured 10 m a.g.l.) between 10 April and 14 May 2019 was mainly easterly. From 12 April onwards, the wind was mainly from the W and WSW. At midday on 21 April, the wind changed direction to the E. It was not until the evening of 24 April that the wind changed direction to the W, and by the evening of 25 April the wind direction oscillated between W and NNW. Similar meteorological conditions occurred on the evening of 28 April and lasted until the end of 29 April, with the wind direction changing between WSW and NNW. The wind direction in May was mainly easterly and only for half a day on 2 and 14 May did the wind blow from a westerly direction (SW to NNW).

In April 2019, Iceland was affected by several local and nonlocal dust events. In particular, between 7 and 12 April, there were daily dust plumes among the south and west coast of Iceland, several hundred km long and visible in true color on Moderate Resolution Imaging Spectroradiometer (MODIS). Additional dust plumes are visible on 16 and 25 April. Dust PM_{10} concentrations in Reykjavik reached up to 300 mg/m^3 on 10–12 April, while $PM_{10} > 100 \text{ mg/m}^3$ were measured also on 22, 25, and 27–28 April, and 12 and 14 May. The measurement station in Akureyri, North Iceland, reported dust concentration $> 800 \text{ mg/m}^3$ on 16 April and $> 600 \text{ mg/m}^3$ on March 26. Dust PM_{10} concentrations in Akureyri exceeded $>100 \text{ mg/m}^3$ also on 27 and 29 March, and 4, 7–9, 11–13, and 24 April. Iceland was affected by a Saharan dust intrusion on 25 April when concentrations from available stations in Reykjavik (Akureyri) were four times (three times) higher than the annual mean. All PM_{10} data are from the Icelandic Air Quality Information System.

3.4. Markers of Icelandic Dust Arriving at Hornsund

In order for a certain particle type to be a marker of a specific source region, it is necessary that it is present exclusively at that place. In the case of Iceland, as plagioclases and metal oxides are also present in the surface sediments at Hornsund, and since augite is chemically similar to the chlorites of local soils, the only phase characterizing the Icelandic origin is volcanic glass. The effective abundance of this phase in many Icelandic sedimentary formations and aeolian dust [29] confirms the hypotheses advanced in our previous studies on the typology and effectiveness of mineralogical records of Icelandic origin in Svalbard aerosols [4,19].

In the graphs of Figure 7, some irregular-shaped particles from the Hornsund aerosols sampled between 14 and 17 April lie in the range of glass particles. This period fits our data on air mass transport from Iceland to Hornsund (Figure 9) and immediately preceding dust events in Iceland. This fact would demonstrate the possibility that Icelandic volcanic sediments raised during dust storms could reach Svalbard through atmospheric circulation. It is noteworthy, however, that some aerosol particles sampled on dates different from 14 and 17 April, in which the presence of direct contributions from Iceland cannot be argued when looking at backward trajectory analysis plus Iceland dust events, appear chemically similar to glass. This fact can be explained by assuming that the particles arriving from Iceland may have remained suspended in the troposphere for some time before reaching the ground due to, e.g., persistent atmospheric stability. That would be in accordance with the very slow movement and narrow circular paths of the air masses a few days before reaching Hornsund on 23 and 24 April. Otherwise, we should conclude that the geochemical interval pertaining to the glass within the graph can be shared by different types of silicate particles including volcanic glass, and that, therefore, the graph is not able to discriminate among the possible silicate components of the aerosols. A similar conclusion has already been reached in the case of pyroxenes with respect to metal particles and chlorites.

A further aspect that emerges from the examination of the graphs is the existence in the aerosols of indeterminate particles, i.e., particles not attributable to the types found in the local and Icelandic soils. These particles with intermediate to aluminiferous composition lie in the central part and to the right corner of the plots, respectively (Figure 7). The

particles with intermediate composition are more frequent in the May samples, while the more aluminiferous ones are present only in the April samples. This does not appear to be due to external mixing effects occurring during long-range transport, as this generally involves the accumulation of alkali sulfate and chloride particles and these could slightly modify the composition of the particles reported in the ternary diagrams we elaborated. In light of our information on the origin of the air masses, and since Greenland is completely snow-capped in the period of interest, we can therefore hypothesize that the first particle type comes from the Siberian area, while the others are more indicative of Northern Europe. In the absence of a database of the composition of surface sediments (including soils) in Eurasia, it is not possible to speak more precisely about the nature and origin of these particles. What is certain is that the graphs show an abrupt change in the composition of aerosols between April and May, and that this change reflects the change in origin of the air masses. In particular, and for the specific purposes of this study, the volcanic glass particles occur in a certain region within the graphs. This may, however, remain a nondiagnostic feature if it is not considered in conjunction with particle morphology.

4. Conclusions

This study used an integrated morphological and chemical particle analysis and meteorological approach to assess the likelihood of Icelandic dust presence in Arctic aerosols. The chemical composition and morphology of particles from aerosol samples collected at Hornsund were analyzed and compared with local and Icelandic surface sediments, assumed to be probable mineral dust sources. The reason for that assumption was the past reports of local natural dust contributing to aerosol and precipitation composition in Svalbard, a previous report of Icelandic dust detection in Ny-Ålesund, Svalbard, and the season of sample collection being a time of frequent dust storm occurrence in Iceland. Iceland is also the most prominent high-latitude dust source in the High Arctic [3].

The mineralogical composition of the loose sediment formations from Iceland and Hornsund exhibited similar points in minor components. Therefore, finding a clear chemical tracer of Icelandic dust was challenging. However, volcanic glass resulted as the best candidate, as hypothesized before [4,19]. An important argument for its use as a tracer was also that volcanic glass is a principal constituent of surface sediments in desert areas in Iceland. The chemical composition and morphology of particles from Hornsund aerosol samples indicate that their dominant part was related to common metamorphic rock sources, while some could be derived from mafic rocks, including volcanic glass. The occurrence of Hornsund aerosol particles with volcanic-glass-like chemical composition in April coincided with more frequent backward air-mass trajectory passing through Iceland and the date of great dust storms in Iceland. We interpret it as an increased likelihood that such particles in Hornsund air originated from Iceland. However, a different source region for particles with similar chemical composition cannot be excluded (e.g., from basalts located elsewhere in the Arctic and sub-Arctic).

For screening potential sources, ternary geochemical diagrams provide a valuable tool for distinguishing likely components of the atmospheric aerosol in the Arctic. However, the analysis may not be conclusive when the number of particles delivered from a particular source is small. Future studies would benefit from expanding the knowledge on the geochemical characteristics of geological substratum across the Arctic. Furthermore, the combined quantitative evaluation of particle morphological characteristics would significantly contribute to the identification of glass particles in atmospheric dust.

Author Contributions: Conceptualization, B.M.; methodology, B.M.; software, S.C.; validation, S.C. and B.M.; samplings, B.M., P.D.W. and D.C.; SEM-EDS analyses, B.M.; investigation, B.M. and S.C.; data curation, B.M. and S.C.; writing—original draft preparation, B.M.; writing—review and editing, B.M., A.N., S.C. and P.D.W.; funding acquisition, D.C. All authors have read and agreed to the published version of the manuscript.

Funding: The study was performed within the “Anthropocene” Priority Research Area under the “Excellence Initiative—Research University” programme. This research has been partially funded by the University of Perugia Research Action no. 5 “Climate, Energy, and Mobility”. The support from the Polish Ministry of Education and Science Project No. DIR/WK/201805 for the Polish Polar Station Hornsund is also acknowledged. The work was partly funded by the Czech Science Foundation (20-06168Y) and Orkurannsóknasjóður (National Power Agency of Iceland).

Institutional Review Board Statement: Not applicable.

Informed Consent Statement: Not applicable.

Data Availability Statement: The data presented in this study are available on request from the corresponding author. The data are not publicly available due to privacy.

Acknowledgments: The staff of the Institute of Geophysics PAS and the Polish Polar Station Hornsund (PPSH) are thanked for establishing and maintaining the meteorological monitoring and support during fieldwork. Special thanks go to K. Koziol for sharing the aerosol samples and sampling information. Finally, we thank M. Michalik for the critical review and K. Koziol for the valuable contribution in both editing and discussion.

Conflicts of Interest: The authors declare no conflicts of interest.

References

- Meinander, O.; Dagsson-Waldhauserova, P.; Amosov, P.; Aseyeva, E.; Atkins, C. Newly identified climatically and environmentally significant high-latitude dust sources. *Atmos. Chem. Phys.* **2022**, *22*, 11889–11930. [[CrossRef](#)]
- Groot Zwaaftink, C.D.; Arnalds, O.; Dagsson-Waldhauserova, P.; Eckhardt, S.; Prospero, J.M.; Stohl, A. Temporal and spatial variability of Icelandic dust emission and atmospheric transport. *Atmos. Chem. Phys.* **2017**, *17*, 10865–10878. [[CrossRef](#)]
- Groot Zwaaftink, C.D.; Grythe, H.; Skov, H.; Stohl, A. Substantial contribution of northern high-latitude sources to mineral dust in the Arctic. *J. Geophys. Res. Atmos.* **2016**, *121*, 13678–13697. [[CrossRef](#)] [[PubMed](#)]
- Moroni, B.; Arnalds, O.; Dagsson-Waldhauserova, P.; Crocchianti, S.; Vivani, R.; Cappelletti, D. Mineralogical and chemical records of Icelandic dust sources upon Ny-Ålesund (Svalbard Islands). *Front. Earth Sci.* **2018**, *6*, 187. [[CrossRef](#)]
- IPCC. *IPCC Special Report on the Ocean and Cryosphere in a Changing Climate*; Pörtner, H.-O., Roberts, D.C., Masson-Delmotte, V., Zhai, P., Tignor, M., Poloczanska, E., Mintenbeck, K., Alegria, A., Nicolai, M., Okem, A., et al., Eds.; Cambridge University Press: Cambridge, UK; New York, NY, USA, 2019; 755p.
- Crocchianti, S.; Moroni, B.; Waldhauserová, P.D.; Becagli, S.; Severi, M.; Traversi, R.; Cappelletti, D. Potential source contribution function analysis of high latitude dust sources over the Arctic: Preliminary results and prospects. *Atmosphere* **2021**, *12*, 347. [[CrossRef](#)]
- Varga, G.; Dagsson-Waldhauserová, P.; Gresina, F.; Helgadóttir, A. Saharan dust and giant quartz particle transport towards Iceland. *Sci. Rep.* **2021**, *11*, 11891. [[CrossRef](#)]
- Kylling, A.; Groot Zwaaftink, C.D.; Stohl, A. Mineral dust instantaneous radiative forcing in the Arctic. *Geophys. Res. Lett.* **2018**, *45*, 4290–4298. [[CrossRef](#)]
- Baldo, C.; Formenti, P.; Nowak, S.; Chevaillier, S.; Cazaunau, M.; Pangui, E.; Di Biagio, C.; Doussin, J.-F.; Ignatyev, K.; Dagsson-Waldhauserova, P.; et al. Distinct chemical and mineralogical composition of Icelandic dust compared to northern African and Asian dust. *Atmos. Chem. Phys.* **2020**, *20*, 13521–13539. [[CrossRef](#)]
- Boy, M.; Thomson, E.S.; Acosta Navarro, J.-C.; Arnalds, O.; Batchvarova, E.; Bäck, J.; Berninger, F.; Bilde, M.; Brasseur, Z.; Dagsson-Waldhauserova, P.; et al. Interactions between the atmosphere, cryosphere, and ecosystems at northern high latitudes. *Atmos. Chem. Phys.* **2019**, *19*, 2015–2061. [[CrossRef](#)]
- Kavan, J.; Stuchlík, R.; Hanáček, M.; Stringer, C.D.; Roman, M.; Holuša, J.; Dagsson-Waldhauserová, P.; Láska, K.; Nývlt, D.; Carrivick, J.L. Proglacial lake evolution coincident with glacier dynamics in the frontal zone of Kvíárjökull, south-east Iceland. *Earth Surf. Process. Landf.* **2024**; *accepted*. [[CrossRef](#)]
- Arnalds, O.; Dagsson-Waldhauserová, P.; Olafsson, H. The Icelandic volcanic aeolian environment: Processes and impacts—A review. *Aeolian Res.* **2016**, *20*, 176–195. [[CrossRef](#)]
- Butwin, M.K.; von Löwis, S.; Pfeffer, M.; Thorsteinsson, T. The Effects of Volcanic Eruptions on the Frequency of Particulate Matter Suspension Events in Iceland. *J. Aerosol Sci.* **2019**, *128*, 99–113. [[CrossRef](#)]
- Dagsson-Waldhauserova, P.; Arnalds, O.; Olafsson, H. Long-term variability of dust events in Iceland. *Atmos. Chem. Phys.* **2014**, *14*, 13411–13422. [[CrossRef](#)]
- Nakashima, M.; Dagsson-Waldhauserová, P. A 60 year examination of dust day activity and its contributing factors from ten Icelandic weather stations from 1950 to 2009. *Front. Earth Sci.* **2019**, *6*, 245–252. [[CrossRef](#)]
- Dagsson-Waldhauserova, P.; Arnalds, O.; Olafsson, H.; Skrabalova, L.; Sigurdardottir, G.M.; Branis, M.; Hladil, J.; Skala, R.; Navratil, T.; Chadimova, L.; et al. Physical properties of suspended dust during moist and low-wind conditions in Iceland. *Icel. Agric. Sci.* **2014**, *27*, 25–39.

17. Bullard, J.E. The distribution and biogeochemical importance of high-latitude dust in the Arctic and Southern Ocean-Antarctic regions. *J. Geophys. Res. Atmos.* **2016**, *122*, 3098–3103. [[CrossRef](#)]
18. Baddock, M.C.; Mockford, T.; Bullard, J.E.; Thorsteinsson, T. Pathways of high-latitude dust in the North Atlantic. *Earth Planet. Sci. Lett.* **2017**, *459*, 170–182. [[CrossRef](#)]
19. Moroni, B.; Becagli, S.; Bolzacchini, E.; Busetto, M.; Cappelletti, D.; Crocchianti, S.; Ferrero, L.; Frosini, D.; Lanconelli, C.; Lupi, A.; et al. Vertical profiles and chemical properties of aerosol particles upon Ny-Ålesund (Svalbard Islands). *Adv. Meteorol.* **2015**, *2015*, 292081. [[CrossRef](#)]
20. Nawrot, A.P.; Migala, K.; Luks, B.; Pakszys, P.; Glowacki, P. Chemistry of snow cover and acidic snowfall during a season with a high level of air pollution on the Hans Glacier, Spitsbergen. *Polar Sci.* **2016**, *10*, 249–261. [[CrossRef](#)]
21. Kavan, J.; Laska, K.; Nawrot, A.; Wawrzyniak, T. High Latitude Dust Transport Altitude Pattern Revealed from Deposition on Snow, Svalbard. *Atmosphere* **2020**, *11*, 1318. [[CrossRef](#)]
22. Spolaor, A.; Moroni, B.; Luks, B.; Nawrot, A.; Roman, M.; Larose, C.; Stachnik, Ł.; Bruschi, F.; Koziol, K.; Pawlak, F.; et al. Investigation on the sources and impact of trace elements in the annual snowpack and the firn in the Hansbreen (Southwest Spitsbergen). *Front. Earth Sci.* **2021**, *8*, 536036. [[CrossRef](#)]
23. Koziol, K.; Uszczyk, A.; Pawlak, F.; Frankowski, M.; Polkowska, Z. Seasonal and Spatial Differences in Metal and Metalloid Concentrations in the Snow Cover of Hansbreen, Svalbard. *Front. Earth Sci.* **2021**, *8*, 538762. [[CrossRef](#)]
24. Cappelletti, D.; Ežerinskis, Ž.; Šapolaitė, J.; Bučinskas, L.; Luks, B.; Nawrot, A.; Larose, C.; Tuccella, P.; Gallet, J.C.; Crocchianti, S.; et al. Long-range transport and deposition on the Arctic snowpack of nuclear contaminated particulate matter. *J. Hazard Mater.* **2023**, *452*, 131317. [[CrossRef](#)]
25. Karasiński, G.; Posyniak, M.; Bloch, M.; Sobolewski, P.; Małarzewski, Ł.; Soroka, J. Lidar Observations of Volcanic Dust over Polish Polar Station at Hornsund after Eruptions of Eyjafjallajökull and Grímsvötn. *Acta Geophys.* **2014**, *62*, 316–339. [[CrossRef](#)]
26. Burakowska, A.; Kubicki, M.; Mysłek-Laurikainen, B.; Piotrowski, M.; Trzaskowska, H.; Sosnowiec, R. Concentration of ⁷Be, ²¹⁰Pb, ⁴⁰K, ¹³⁷Cs, ¹³⁴Cs radionuclides in the ground layer of the atmosphere in the polar (Hornsund, Spitsbergen) and mid-latitudes (Otwock-Świder, Poland) regions. *J. Environ. Radioact.* **2021**, *240*, 106739. [[CrossRef](#)] [[PubMed](#)]
27. Kepski, D.; Luks, B.; Migala, K.; Wawrzyniak, T.; Westermann, S.; Wojtuń, B. Terrestrial Remote Sensing of Snowmelt in a Diverse High-Arctic Tundra Environment Using Time-Lapse Imagery. *Remote Sens.* **2017**, *9*, 733. [[CrossRef](#)]
28. Đorđević, D.; Tošić, I.; Sakan, S.; Petrović, S.; Đuričić-Milanković, J.; Finger, D.C.; Dagsson-Waldhauserová, P. Can Volcanic Dust Suspended From Surface Soil and Deserts of Iceland Be Transferred to Central Balkan Similarly to African Dust (Sahara)? *Front. Earth Sci.* **2019**, *7*, 142–154. [[CrossRef](#)]
29. Baratoux, D.; Mangold, N.; Arnalds, O.; Bardintzeff, J.-M.; Platevoet, B.; Grégoire, M.; Pinet, P. Volcanic sands of Iceland—Diverse origins of aeolian sand deposits revealed at Dyngjúsandur and Lambhraun. *Earth Surf. Proc. Land.* **2011**, *36*, 1789–1808. [[CrossRef](#)]
30. Birkenmajer, K. *Geology of the Hornsund Area, Spitsbergen. Map 1:75000 and Explanations*; Uniwersytet Śląski: Katowice, Poland, 1990.
31. Birkenmajer, K. Precambrian succession at Hornsund, south Spitsbergen: A lithostratigraphic guide. *Studia Geol. Pol.* **1992**, *98*, 7–66.
32. Majka, J.; Mazur, S.; Manecki, M.; Czerny, J.; Holm, D. Late Neoproterozoic amphibolite-facies metamorphism of a pre-Caledonian basement block in southwest Wedel Jarlsberg Land, Spitsbergen: New evidence from U–Th–Pb dating of monazite. *Geol. Mag.* **2008**, *145*, 822–830. [[CrossRef](#)]
33. Majka, J.; Czerny, J.; Mazur, S.; Holm, D.K.; Manecki, M. Neoproterozoic metamorphic evolution of the Isbjørnhamna Group rocks from south-western Svalbard. *Polar Res.* **2010**, *29*, 250–264. [[CrossRef](#)]
34. Czerny, J.; Kieres, A.; Manecki, M.; Rajchel, J. *Geological Map of the SW Part of Wedel Jarlsberg Land, Spitsbergen 1:25000*; Manecki, A., Ed.; Institute of Geology and Mineral Deposits, University of Mining and Metallurgy: Cracow, Poland, 1993; pp. 1–61.
35. Stein, A.F.; Draxler, R.R.; Rolph, G.D.; Stunder, B.J.B.; Cohen, M.D.; Ngan, F. NOAA's HYSPLIT Atmospheric Transport and Dispersion Modeling System. *Bull. Am. Meteorol. Soc.* **2015**, *96*, 2059–2077. [[CrossRef](#)]
36. Moroni, B. Morphochemical Characteristics and Mixing State of Icelandic Dust. Scientific Report. COST Project Action Number: CA16202 STSM. 2020. Available online: https://earth.bsc.es/indust/lib/exe/fetch.php?media=public:stsm-scientific-report_moroni_rev.pdf (accessed on 10 October 2023).

Disclaimer/Publisher's Note: The statements, opinions and data contained in all publications are solely those of the individual author(s) and contributor(s) and not of MDPI and/or the editor(s). MDPI and/or the editor(s) disclaim responsibility for any injury to people or property resulting from any ideas, methods, instructions or products referred to in the content.